

The Evolutionary Ecology of Individual Foraging Decisions

Pratik R. Gupte^{1,*}

Christoph F. G. Netz¹

Franz J. Weissing¹

1. University of Groningen, Groningen 9747AG, The Netherlands.

* Corresponding authors; e-mail: p.r.gupte@rug.nl

Manuscript elements: EXAMPLE: Figure 1, figure 2, table 1, online appendices A and B (including figure A1 and figure A2). Figure 2 is to print in color.

Keywords: Examples, model, template, guidelines.

Manuscript type: Article.

Prepared using the suggested L^AT_EX template for *Am. Nat.*

Abstract

Understanding the causes and consequences of animal movement is key to mechanistically linking individual behaviour with population-level patterns. Classical models of individual-to-population foraging distributions do not account for the complex and changeable resource landscapes animals must navigate. Neither are the rich behavioural repertoires addressed that animals may exhibit in a foraging context, and their evolution is almost entirely ignored. We take a spatially explicit, individual-based simulation approach to model the evolution of individual movement and foraging strategies, and its consequences for population distributions in three simple foraging scenarios of increasing behavioural complexity. We show that movement rules and individual foraging strategies co-evolve to optimality in all three scenarios. We find that exploitation competition is a relatively weak driver of individual movement and intake, and that this effect depends on the replenishment rate of the resource. We also find that when interference competition in the form of kleptoparasitism is allowed, it gives rise to a quasi-predator class of individuals and a third trophic level emerges. These quasi-predators compete among themselves much more than they compete with all other individuals, even when they are able to switch from a scrounger to a producer strategy.

WIP.

Introduction

Evolutionary Simulation Model of Individual Foraging Decisions

Our model is an individual-based evolutionary simulation whose most basic components — the environment size and shape, its gridded structure and each cell’s capacity to hold multiple individuals, as well as the discrete conception of time within and between generations — is taken from Netz et al. *in prep.*. We conceptualised the model and the scenarios around the behaviour of waders (*Charadrii*, and especially oystercatchers *Haematopus sp.*), which are extensively studied in an optimal foraging context (e.g. Ens et al., 1990; Vahl et al., 2005a,b,c). We simulated a fixed population with a fixed size of 10,000 individuals moving on a landscape of 512^2 grid cells, with the landscape wrapped at the boundaries so that individuals passing beyond the bounds at one end re-appear on the diametrically opposite side. Individuals have a lifetime of T timesteps, with T set to 400 by default. After their lifetime, individuals reproduce and transmit their heritable traits proportional to their fitness over their lifetime. The model code (in C++) can be found as part of the Supplementary Material in the Zenodo repository at **Zenodo/other repository here**.

Flexibility in Foraging Strategies

Our model considers three main scenarios of flexibility in individual foraging strategies. The **first scenario** is an inflexible producer-only case, in which individuals move about on the landscape and probabilistically find and consume discrete prey food items. Between finding and consuming a food item, individuals must ‘handle’ the prey for a fixed handling time T_H which is constant across prey items. Prey handling time T_H is set at 5 timesteps by default. The handling time dynamic is well known from many systems; for instance, it could be the time required for a wader to break through a mussel shell, with the handling action obvious to nearby individuals, and the prey not fully under the control of the finder. We refer to such individuals as ‘handlers’ for convenience. Handlers are assumed to be fully absorbed in their processing of prey, and do

not make any movements until they have fully handled and consumed their prey. The **second scenario** is a fixed-strategy case which adds some flexibility. Individuals at the start of their lifetime each choose between two foraging strategies, which are then fixed through life. The strategy choice is based on local environmental cues, and is covered in “Movement and Foraging Decisions”. The two strategies are to produce, i.e., to probabilistically find, handle, and consume discrete prey (as in the producer-only case), or to scrounge as a kleptoparasite, i.e., to steal a found prey item from the individual handling it. We refer to such scroungers as ‘kleptoparasites’ from here onwards. Kleptoparasites can steal from any handler, regardless of whether that handler acquired its prey by searching or theft. Kleptoparasites are always successful in stealing from the handler they target; this may be thought of as the benefit of the element of surprise, a common observation in nature. Having acquired prey, a kleptoparasite need only handle it for $T_H - t_h$ timesteps, where t_h is the time that the prey has already been handled by its previous handler. The targeted handler deprived of its prey is assumed to flee from the area, and does not make a further movement decision. Thus kleptoparasites clearly save time on handling compared to a producer, and the time saved increases with the handling time T_H of the prey. The **third scenario** is a flexible-strategy case, and individuals are allowed to be plastic in their foraging strategies, and choose between producing and scrounging strategies in each timestep. Apart from the frequency of the choice, the actual foraging dynamics are the same as described in the fixed-strategy case. Individuals move about on the environment, and each foraging strategy choice is based on local environmental cues (see “Movement and Foraging Decisions”).

Movement and Foraging Decisions

Individuals essentially use cues available in timestep t to predict their best move for the next timestep $t + 1$, and the strategy associated with that move (when this is allowed). The movement decision is based on three local environmental cues: (1) the number of discrete prey items G , (2) the number of individuals handling prey H (referred to as ‘handlers’), and (3) the number of individuals not handling prey P (referred to as ‘non-handlers’). The notation is chosen in keeping

with Netz et al. *in prep.*. These cues are available to individuals in all three model scenarios. Individuals occupy a single grid cell on the environment at a time, and assign a suitability score S incorporating G , H , and P per cell to the nine cells in their Moore neighbourhood (including their current cell). Following Netz et al. *in prep.*, individuals calculate the cell-specific S as

$$S = m_g G + m_h H + m_p P + m_b$$

where the weighing factors for each cue m_g , m_h and m_p , and the bias m_b are genetically encoded and heritable between generations. Individuals rank their Moore neighbourhood by S in timestep t and move to the highest ranked cell in timestep $t + 1$.

Individuals in the producers-only case make no foraging decisions and find food items probabilistically (see “Prey Environment and Ecological Dynamics”). In the fixed-strategy case, individuals pick a lifelong foraging strategy in their first timestep (t_0), while in the flexible-strategy case, individuals pick a strategy in each timestep t to be deployed in $t + 1$. Individuals in these latter two cases process the cell-specific environmental cues G , H , and P to determine their foraging strategy F for life (fixed strategy), or in the grid cell into which they have chosen to move in $t + 1$ (flexible strategy). F is determined as

$$F = \begin{cases} \text{producer,} & \text{if } f_g G + f_h H + f_p P + f_b \geq 0 \\ \text{scrounger,} & \text{otherwise} \end{cases}$$

where the cue weights f_g , f_h and f_p , and the bias f_b are also genetically encoded and heritable between generations.

In both latter cases that allow for kleptoparasitism, individuals make their foraging strategy choice for the next timestep after they have passed through the ecological dynamics of their current location. This excludes individuals that have been stolen from are an important exception; these fleeing agents are moved to a random cell within a Chebyshev distance of 5, and do not make a foraging decision there. Thus kleptoparasitism not only gains individuals prey items while depriving the targeted individual, it also displaces a potential competitor. All individu-

als move simultaneously, and attempt to implement the foraging strategy chosen for their new location (see below).

Prey Environment and Ecological Dynamics

Since our model was initially conceived to represent foraging waders, we developed a resource landscape based on mussels (family *Mytilidae*) that are commonly found in inter-tidal systems. Mussels beds share some important characteristics with other discrete prey items. Firstly, mussels are immobile relative to their consumers, and their abundances are largely driven by extrinsic environmental gradients and very small-scale interactions (de Jager et al., 2020, 2011). Secondly, in common with many ecological systems (Levin, 1992), mussels are not uniformly distributed across the inter-tidal mudflats, and are instead strongly spatially patterned into clusters (‘beds’) (de Jager et al., 2020, 2011). Thirdly, while prey or their signs in an area are often visible to consumers, consumers are not always certain of obtaining one of these prey, since prey can show small-scale anti-predator avoidance responses.

We captured these essential aspects of prey dynamics when implementing the resource landscape on which our individuals move. We modelled relative prey immobility and extrinsically driven abundance by assigning each grid cell of the resource landscape a constant probability of generating a new prey item per timestep, which we refer to as the growth rate r . We modelled clustering in the abundance of prey by having the distribution of r across the grid cells take the form of 1,024 uniformly distributed resource peaks with r declining from the centre of each peak to its periphery (Figure X). Effectively, the cell at the centre of each patch generates a prey item five times more frequently than the cells at the edges. Thus for a simulation-specific baseline $r_{base} = 0.03$, the central cell of a resource peak would have an $r_{centre} = 0.03$, and generate 3 items every 100 timesteps, compared with $r_{edge} = 0.006$, or 0.6 items generated in 100 timesteps. We ran the simulation with r_{base} values of 0.001, 0.01, 0.03, and 0.05, which we considered a sufficiently broad range. Cells in our landscape were modelled as being able to hold a maximum of K prey items, with the default $K = 5$. While a cell is at carrying capacity its r is 0. We modelled near-

perfect intermediate-range perception but uncertain short-range acquisition of prey by allowing individuals to perceive all prey items G in a cell, but giving individuals which choose a producer strategy only a probability of finding one of these prey. The probability of finding a prey item $p(success)$ is given as the probability of not finding any of G prey

$$p(success) = 1 - (1 - p_i)^G$$

where p_i is the detection probability of each of G items, which is uniformly set to 0.2 by default for all items.

Since we model foraging events as occurring simultaneously, it is possible for more producers to be considered successful in finding prey than there are discrete items in that cell. We resolve this simple case of exploitation competition by assigning G prey among some N successful finders at random. Producers that are assigned a prey item in timestep t begin handling it, and are considered to be handlers for the purposes of timestep $t + 1$ (primarily movement and foraging decisions of other individuals). It is important to note that a producer that has converted into a handler in timestep t is not an available target for kleptoparasites until timestep $t + 1$. Producers that are not assigned a prey item are considered idle during timestep t , and are counted as non-handlers for $t + 1$.

Kleptoparasites in the fixed- or flexible-strategy case face a slightly different challenge. All kleptoparasites in a cell successfully steal from a handler, contingent on the number of handlers matching or exceeding the number of kleptoparasites in timestep t . When the number of kleptoparasites exceeds handlers, handlers are assigned among kleptoparasites at random. Successful kleptoparasites convert into handlers, and similar to producer-handlers are unavailable as targets to other kleptoparasites until the next timestep. Unsuccessful kleptoparasites are considered idle, and are also counted as non-handlers for timestep $t + 1$. A handler that finishes processing its prey in timestep t returns to the non-handler state and is assessed as such by other agents when determining movements for $t + 1$.

Individuals move and forage on the resource landscape for T timesteps per generation, and

T is set at 400 by default. Handling a food item requires a maximum of T_H timesteps, during which the handler is immobile.

Reproduction and the Evolution of Decision Making

At the end of each generation, the population is replaced by its offspring, maintaining the fixed population size, and the decision-making weights which determine individual movement (m_g, m_h, m_p, m_b) and foraging strategy choice (f_g, f_h, f_p, f_b) are transmitted from parent individuals to offspring. The number of offspring of each parent is proportional to the parent's share of the population fitness, and this is implemented as a weighted lottery that selects a parent for each offspring. The total lifetime intake of individuals is used as a proxy of fitness, and the population's total fitness is its total intake. The decision-making weights are subject to independent random mutations with a probability of 0.001. The size of the mutation (either positive or negative) is drawn from a Cauchy distribution with a scale of 0.01 centred on the current value of the weight to be mutated. This allows for a small number of very large mutations while the majority of mutations are small. Autocorrelation in the landscape coupled with limited natal dispersal can lead to spatial heterogeneity becoming fixed in populations, as lineages adapt to local conditions. Among other things, this could lead to population-level movements due to differential reproduction that mirror shifts in resource abundance, rather than individual movement. To ensure individual movement rules evolved, we initialised each offspring at a random location on the landscape, and also reset its total intake to zero.

Simulation Output and Analysis

Spatial Distribution of Individuals, their Intake, and Prey Items. Over each of the last eight generations of the simulation (991 – 998), we summed the following for each grid cell ij over the generation's timesteps: (1) the number of prey items G , (2) the number of individuals following each of the two strategies, producer N_p or kleptoparasitic scrounger N_s , and (3) the intake (in

food items consumed after handling) by agents following each of the two strategies, producer I_p or kleptoparasite I_s . For instance, the number of producer individuals in a generation to inhabit a cell ij would be

$$N_p = \sum_{t=0}^{i=T} n_{p_t}$$

where $t \in (0, 1 \dots T = 400)$, and n_{p_t} is the number of producers in cell ij at each timestep t . We saved this generation- and simulation- specific data to file, and these data are available at the Zenodo/IRODS repository at **Zenodo/other link here**. The volume of data at this stage was comparable to a very high-resolution, long-term ecological study, and we handled it accordingly. First, we processed the data to get the timestep-averaged values of G , N_p , N_s , I_p , and I_s for each cell, dividing each value by T (400). From this data, we calculated the per-capita intake rate (I per t) on each cell for each of the two strategies separately, which we denote as R_p (producers) and R_s (scroungers). We plotted the timestep- and generation-averaged item count (G), strategy count (N_p , N_s), and absolute and per-capita intake (I_p , I_s , and R_p , R_s) in relation to grid-cell quality (the growth rate, r) to investigate the spatial distribution of individuals (see Figure X).

Generalised Functional Response. In our simulation, individuals perceive and respond to the standing stock of prey items G on a cell rather than its growth rate r . This standing stock is unpredictable due to consumption by other individuals. To understand the consequences of movement, we need to investigate how individual intake rate varies with G as well as the presence of potential competitors. Thus we examined the generalised functional response (W) *sensu* Meer and Ens (1997). We plotted the per-capita intake rate achieved by individuals on grid-cells with similar numbers of prey items (G) and individuals ($N_p + N_s$) (see Figure Xa). We did this separately for W_p and W_s , the generalised functional response of individuals using the producer and kleptoparasitic scrounger respectively (see Figure Xb, Xc). We modelled the effect of competition and resource availability on W_p and W_s using a simple generalised linear model (GLM) with either W_p or W_s as the response, and the number of individuals and the number of prey items as the only additive predictors. We repeated this for simulations with different

baseline growth rates r , and examined variation in the contribution of competition and resource availability in the **form of the linear model coefficients of individual density and item density, respectively (see Figure X)**. These linear models took the form

$$W = \beta_0 + \beta_1 G + \beta_2 (N_p + N_s)$$

where W is either W_p or W_s . We fit these models for each r_{base} separately, but did not distinguish between replicates.

Decision Making Weights. To understand the evolutionary consequences of our simulation, we exported the the decision-making weights which determine individual movement (m_g, m_h, m_p, m_b) and foraging strategy choice (f_g, f_h, f_p, f_b) of each individual in every generation of the simulation. We examined how the frequency of these weights changed over the simulation, i.e., how the weights evolved. We visualised weights' evolution after scaling them between -1 and +1 using a hyperbolic tangent function, and binning the scaled values into intervals of 0.1. We refer to these scaled and binned values as phenotypes for convenience. Weights at or near -1 would represent the maximum evolved avoidance of an environmental cue (in relation to a movement weight) or the greatest evolved negative effect of a cue on choosing the foraging strategy (in relation to a strategy choice weight). Similarly, weights at or near +1 represent the greatest evolved preference for or positive effect of a cue on the movement and strategy choice mechanism of an individual.

Simulation Model Outcomes

Emergence of a Dynamic Equilibrium

WIP.

Evolution of Decision Making Weights

Scenario 1: The Producers-Only Case. Among the weights determining movement, the weight for food items m_g evolved consistently positive values across values of r_{base} but the population did not converge upon a single value of m_g (see Figure X). The number of phenotypes expressed by $\geq 1\%$ of the population declined asymptotically over generations, and there were fewer such phenotypes at lower r_{base} . The phenotypes expressed were not consistent across replicate simulations with the same r_{base} . The weight for handlers m_h evolved mostly positive values over the range of r_{base} , but this weight too did not converge upon a single value, evolving neutrally for $r_{base} \geq 0.075$ (Figure X). Negative values of m_h also evolved repeatedly and persisted for multiple generations when $r_{base} < 0.1$. The number of phenotypes of m_h declined asymptotically over evolutionary time up to an r_{base} of 0.1, after which they appeared to decline linearly. Simulations with lower r_{base} also had fewer m_h phenotypes. The weight for non-handlers m_p evolved consistently negative values for $0.001 \leq r_{base} \leq 0.04$, but did not converge to a single value. For $r_{base} \in 0.05, 0.075$, m_p evolved negative or neutral values in different replicates, while for $r_{base} \geq 0.1$ m_p evolved neutrally (Figure X).s The number of phenotypes of m_p declined asymptotically over evolutionary time up to an r_{base} of 0.1, after which they appeared to decline linearly. Simulations with lower r_{base} also had fewer m_p phenotypes in general (Figure X). The four decision making weights for foraging strategy (f_g, f_h, f_p, f_b) evolved neutrally since individual foraging strategies were fixed to searching for food, i.e., being a producer (see Figure X). Nonetheless, the number of phenotypes declined asymptotically over generations, but there were no differences in relation to r_{base} .

Scenario 2: The Fixed Strategy Case. Of the movement weights, the weight for food items m_g evolved consistently positive values for all r_{base} except 0.25, where m_g evolved neutrally across the positive range. Furthermore, the population largely converged upon m_g values close to zero, though variation in m_g persisted over evolutionary time for all r_{base} . This was reflected in the

number of m_g phenotypes which declined asymptotically nearly to zero over generations with
 little difference among r_{base} , except for $r_{base} = 0.25$ which showed a weakly linear decline. The
 weight for handlers m_h evolved with little consistency in direction or magnitude, with mostly
 positive values for $r_{base} \leq 0.01$, and a mixture of positive and negative values beyond that.
 Rather than converge to a single m_h , the population expressed a few distinct m_h phenotypes
 over generations, with multiple phenotypes of similar population frequencies co-existing in the
 same generation. Consequently, the number of m_h phenotypes remained almost constant after
 an initial asymptotic decline over generations, with no differences among r_{base} except for $r_{base} =$
 0.25 which showed a weakly linear decline. The weight for non-handlers m_p evolved consis-
 tently negative values over r_{base} but rather than converge to a single m_p , the population showed
 a few distinct m_p phenotypes over generations, and multiple phenotypes of similar population
 frequencies co-existed in the same generation. At the highest r_{base} (0.25) m_p evolved neutrally
 (Figure X). The number of phenotypes of m_p declined asymptotically over evolutionary time up
 to an r_{base} of 0.1, after which they declined linearly, but there were no differences among growth
 rates except when $r_{base} = 0.25$. The weights determining the lifetime foraging strategy ($f_g, f_h, f_p,$
 f_b) did not evolve consistently across r_{base} , and showed both large variation as well as coexistence
 of phenotypes of similar frequencies across generations. There was no easily detected pattern
 in the difference among dominant phenotypes. All foraging strategy weights evolved neutrally
 when $r_{base} = 0.25$; the bias f_b evolved neutrally only in the positive range at this growth rate.

Scenario 3: The Flexible Strategy Case. Decision making weights evolved in a pattern contrary
 to the producer-only and fixed-strategy cases, with the population converging to one or a few
 values of all weights at high growth rates, and with more variation at lower growth rates. The
 movement weight for food items m_g evolved to consistently positive values near zero across r_{base} ,
 with convergence on a single phenotype or the maintenance of 1 – 3 phenotypes with decreasing
 r_{base} . The weight for handlers m_h also evolved consistently positive values over different r_{base} ,
 with increasing variation at lower growth rates. Indeed, the lowest variation was seen at inter-

mediate growth rates ($r_{base} \in 0.04, 0.05, 0.075, 0.1$). The weight for non-handlers m_p showed little consistency, and evolved positive values just above zero for $r_{base} = 0.25$, and largely negative or neutral values for all other growth rates. The population showed less convergence in this weight than others, with between 1 – 3 dominant phenotypes in any simulation. Weights determining foraging strategies also showed convergence upon 1 – 3 dominant phenotypes with increasing growth rates, and substantial variation at lower growth rates. While the strategy bias f_b and the strategy weight for non-handlers f_p showed no clear pattern, the strategy weight for handlers f_h evolved consistently negative values at $r_{base} < 0.01$, below which showed more variation in both the positive and negative range (see Figure X). The strategy weight for food f_g almost always converged to values at or near zero for $r_{base} > 0.01$, below which it evolved neutrally. Overall, the sum of strategy weights evolved consistent, strongly negative values for $r_{base} > 0.02$, below which there was more variation.

Spatial Distribution of Individuals and Prey

Individual Distributions. There number of individuals on a cell increased with its growth rate r , but there was substantial variation across cells with the same r . This variation was larger with increasing r since there were fewer cells with higher r . In the producer-only case, individual abundance showed a linear increase with cell quality, with the slope increasing with the simulation growth rate r_{base} . When two strategies were allowed however, there were strong differences in how they were distributed across cell qualities. In the fixed-strategy case, the abundance of producer individuals was uniformly low across cell qualities, while the abundance of scrounging kleptoparasites had a sigmoidal relationship with quality, mediated by r_{base} . In the flexible-strategy case, the use of either strategy was nearly invariant with cell quality. At very low r_{base} (0.001) the kleptoparasitic strategy was more often used than the producer strategy, while at higher r_{base} , the producer strategy was more common across cell quality.

290 *Consequences for Prey Item Distribution.* The distributon of items G varied considerably between
 291 scenarios and simulation-specific baseline growth rates r_{base} . In the **first scenario** G was insensi-
 292 tive to r , and items were uniformly distributed across cells of different growth rates. G was not
 293 significantly different among simulations with different r_{base} . In the **second scenario** G increased
 294 strongly with r , and the curve of $G r$ varied with r_{base} . The $G r$ transformed from roughly linear
 295 ($r_{base} = 0.001$), to exponential ($r_{base} = 0.01$), and finally to sigmoidal ($r_{base} \in 0.03, 0.05$) [see Figure
 296 X]. In the **third scenario** G varied only weakly across cells with different r , and the $G r$ response
 297 had a positive slope only for the highest r_{base} of 0.03 and 0.05.

298 *Generalised Functional Response*

299 The model coefficients of G and $N_p + N_s$ changed non-linearly in relation to r_{base} (Figure X). In
 300 the producers-only case, the coefficient β_2 increased with r_{base} when $r_{base} \leq 0.03$, after which it
 301 decreased below zero for $r_{base} = 0.25$. Similarly, the coefficient of items β_1 was highest at $r_{base} =$
 302 0.03, decreasing to zero for $r_{base} = 0.1$ and 0.25. In the fixed-strategy case, β_1 (items) was at or
 303 near zero across all r_{base} . However, β_2 for both W_p and W_s was near zero for $r_{base} \leq 0.05$, positive
 304 for $r_{base} \in 0.075, 0.1$, and zero for $r_{base} = 0.25$. Both in the flexible-strategy case, both β_1 and β_2
 305 showed a hump-shaped relationship with r_{base} for both W_p and W_s , with the highest values at
 306 intermediate growth rates.

307 **Discussion**

308 **Conclusion**

309 **Acknowledgments**

310 The authors thank Hanno Hildenbrandt for contributing to the coding of the simulation model
 311 *Kleptomove*; Matteo Pederboni for contributing to the initial stages of the simulation model; and
 312 members of the Modelling Adaptive Response Mechanisms Group and of the Theoretical Biology

department at the University of Groningen for helpful discussions on the manuscript.

Literature Cited

de Jager, M., J. van de Koppel, E. J. Weerman, and F. J. Weissing. 2020. Patterning in Mussel Beds Explained by the Interplay of Multi-Level Selection and Spatial Self-Organization. *Frontiers in Ecology and Evolution* 8.

de Jager, M., F. J. Weissing, P. M. J. Herman, B. A. Nolet, and J. van de Koppel. 2011. Lévy Walks Evolve Through Interaction Between Movement and Environmental Complexity. *Science* 332:1551–1553.

Ens, B. J., P. Esselink, and L. Zwarts. 1990. Kleptoparasitism as a problem of prey choice: A study on mudflat-feeding curlews, *Numenius arquata*. *Animal Behaviour* 39:219–230.

Levin, S. A. 1992. The Problem of Pattern and Scale in Ecology: The Robert H. MacArthur Award Lecture. *Ecology* 73:1943–1967.

Meer, J. V. D., and B. J. Ens. 1997. Models of Interference and Their Consequences for the Spatial Distribution of Ideal and Free Predators. *The Journal of Animal Ecology* 66:846.

Vahl, W. K., T. Lok, J. van der Meer, T. Piersma, and F. J. Weissing. 2005a. Spatial clumping of food and social dominance affect interference competition among ruddy turnstones. *Behavioral Ecology* 16:834–844.

Vahl, W. K., J. van der Meer, F. J. Weissing, D. van Dulleman, and T. Piersma. 2005b. The mechanisms of interference competition: Two experiments on foraging waders. *Behavioral Ecology* 16:845–855.

———. 2005c. The mechanisms of interference competition: Two experiments on foraging waders. *Behavioral Ecology* 16:845–855.

335

Appendix A: Supplementary Figures

336

Fox–dog encounters through the ages

337

Appendix B: Additional Methods

338

Measuring the height of fox jumps without a meterstick

Tables

340

Figure legends

341

Online figure legends

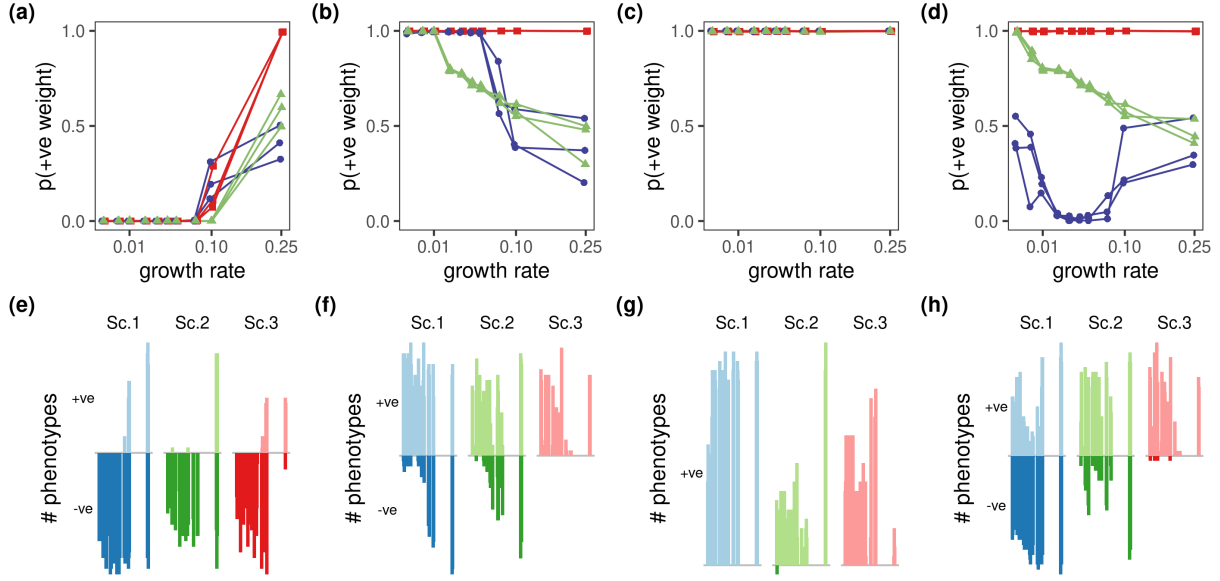


Figure 1: Proportion of individuals in populations evolved across different regrowth rates selecting for environmental cues in deciding movement. Panels (a – d) show the proportion of individuals with positive weights for each cue: (a) non-handling individuals, (b) handling individuals, (c) prey items, and (d) individuals overall. Colours and shapes represent scenarios (blue circles: *producers-only*; green triangles: *fixed-strategy*; red squares: *flexible-strategy*). While lines connect similarly numbered replicates across r_{base} , these are entirely independent simulations. Panels (e – h) show the number of distinct values for each weight in the population in panels (a – d) separated by the sign (positive or negative): (e) non-handling individuals, (f) handling individuals, (g) prey items, and (h) individuals overall. Bar colours represent scenarios (blue: *producers-only*; green: *fixed-strategy*; red: *flexible-strategy*), while the hue represents the sign (light: positive, dark: negative). Individuals avoid non-handlers for $r_{base} \leq 0.1$, after which they evolve neutrally in scenarios 1 and 2, and strongly positive values in scenario 3 (a, e). Similarly, most individuals in scenarios 1 and 2 move towards handlers, but the proportion and diversity of negative weights increases at $r_{base} \geq 0.1$ (b, f). Individuals in scenario 3 consistently move towards handlers, and individuals overall (b, f, d, h). Overall, in scenario 1 individual preference for moving towards other individuals has an inverse-humped relationship with r_{base} , while in scenario 2 it shows a steady linear decline.